LETTERS
PUBLISHED ONLINE: 26 FEBRUARY 2014 | DOI: 10.1038/NCLIMATE2134
nature climate change

Ecological stability in response to warming

Katarina E. Fussmann[1†], Florian Schwarzmüller[1†], Ulrich Brose[1*], Alexandre Jousset[1,2] and Björn C. Rall[1]

That species' biological rates including metabolism, growth and feeding scale with temperature is well established from warming experiments[1]. The interactive influence of these changes on population dynamics, however, remains uncertain. As a result, uncertainty about ecological stability in response under warming remains correspondingly high. In previous studies, severe consumer extinction waves in warmed microcosms[2] were explained in terms of warming-induced destabilization of population oscillations[3]. Here, we show that warming stabilizes predator–prey dynamics at the risk of predator extinction. Our results are based on meta-analyses of a global database of temperature effects on metabolic and feeding rates and maximum population size that includes species of different phylogenetic groups and ecosystem types. To unravel population-level consequences we parameterized a bioenergetic predator–prey model[4] and simulated warming effects within ecological, non-evolutionary timescales. In contrast to previous studies[3], we find that warming stabilized population oscillations up to a threshold temperature, which is true for most of the possible parameter combinations. Beyond the threshold level, warming caused predator extinction due to starvation. Predictions were tested in a microbial predator–prey system. Together, our results indicate a major change in how we expect climate change to alter natural ecosystems: warming should increase population stability while undermining species diversity.

Ongoing global warming is documented in different ecosystems worldwide[5,6]. Such global warming can lower abundances and lead to extinction, for example, due to habitat loss[5,7–9]. However, specific predictions of consequences for global ecosystems and species are still vague, because warming simultaneously affects many levels of ecological organization. This includes simultaneous changes of multiple biological and biochemical rates with temperature[3,10,11]: increased individual metabolic rate[1] and intrinsic population growth[12], as well as modified feeding parameters (maximum feeding and half-saturation density) of predator–prey interactions[10,13,14] (Fig. 1a). Traditionally, severe consumer extinction waves in warmed microcosms[2] were explained by increased metabolic and feeding rates that destabilize population dynamics by causing stronger oscillations[3]. However, the lack of systematic empirical data and their integration with generalized models hampered an understanding of their interactive influence on population dynamics and species survival. Hence, predictions of warming effects on ecosystems and their stability remained highly uncertain. To overcome these limitations, we analysed a new global database and addressed how warming affects metabolic and feeding rates as well as maximum population size across species of different phylogenetic groups and ecosystem types. Subsequently, we used these empirical physio-ecological scaling relationships and parameterized a bioenergetic model to predict warming effects on population stability and species' survival probabilities. We tested these predictions in a microbial microcosm experiment across a temperature gradient. Together, these integrated analyses provide a generalized understanding of how warming affects natural communities.

Temperature dependencies of biological rates (x) are commonly described by the Arrhenius equation (see Fig. 1b with metabolic rates as an example):

$$x_c = x_0 e^{E_x \frac{T-T_0}{kTT_0}} \quad (1)$$

where x_0 is a rate- and mass-dependent normalization constant, E_x (eV) is the rate's activation energy, T is the absolute temperature of the system (K), k (eV K^{-1}) is Boltzmann's constant and T_0 (K) the normalization temperature (here: 20 °C = 293.15 K).

Using a global database, we analysed activation energies for metabolic rates, carrying capacities (maximum density of the prey), maximum feeding rates and half-saturation densities (prey density at which half of the maximum feeding rate is realized, see Fig. 1a, thus expressing the predator's foraging inefficiency), which are parameters of a bioenergetic population model of previous studies[4,15,16]. Values for the intrinsic growth rate of resource populations were 0.84 eV for multicellular organisms with non-overlapping generations[12]. In our analyses, activation energies of the carrying capacity are generally negative, whereas activation energies of the half-saturation density are close to zero (Fig. 1c). This significant difference suggests that predators cannot increase their foraging efficiency to cope with scarcer prey in warmer systems. Moreover, maximum feeding increases significantly less with warming than metabolic rate (lower activation energies, Fig. 1c), which implies that predators in warmer ecosystems suffer from increased energy loss owing to metabolism whereas their maximum energy intake cannot increase similarly. Both significant differences (as indicated in Fig. 1c) suggest a reduced energy supply for predators in a warmed world.

To investigate the interplay of these warming effects with population dynamics, we used the average activation energies and their standard deviations to parameterize a bioenergetic model[17–19] (Methods). We also implemented published data for the temperature dependency of resource population growth[12]. Our initial model simulations were based on the average activation energies (see legend of Fig. 1 and Supplementary Table 1) to predict dynamics along a temperature gradient (0 °–40 °C). We found predator extinctions at low temperatures (<11 °C) due to unstable population dynamics. Predators and prey persisted along a temperature range between 11 °C and 27.5 °C, whereas above 27.5 °C predators became extinct owing to energy limitations (Fig. 2a). Although these temperature thresholds remain specific for

[1]J.F. Blumenbach Institute of Zoology and Anthropology, Georg-August University, Göttingen 37073, Germany, [2]Ecology and Biodiversity, Department of Biology, Utrecht University, Padualaan 8, 3584 CH Utrecht, the Netherlands. †These authors contributed equally to this work. *e-mail: ubrose@gwdg.de

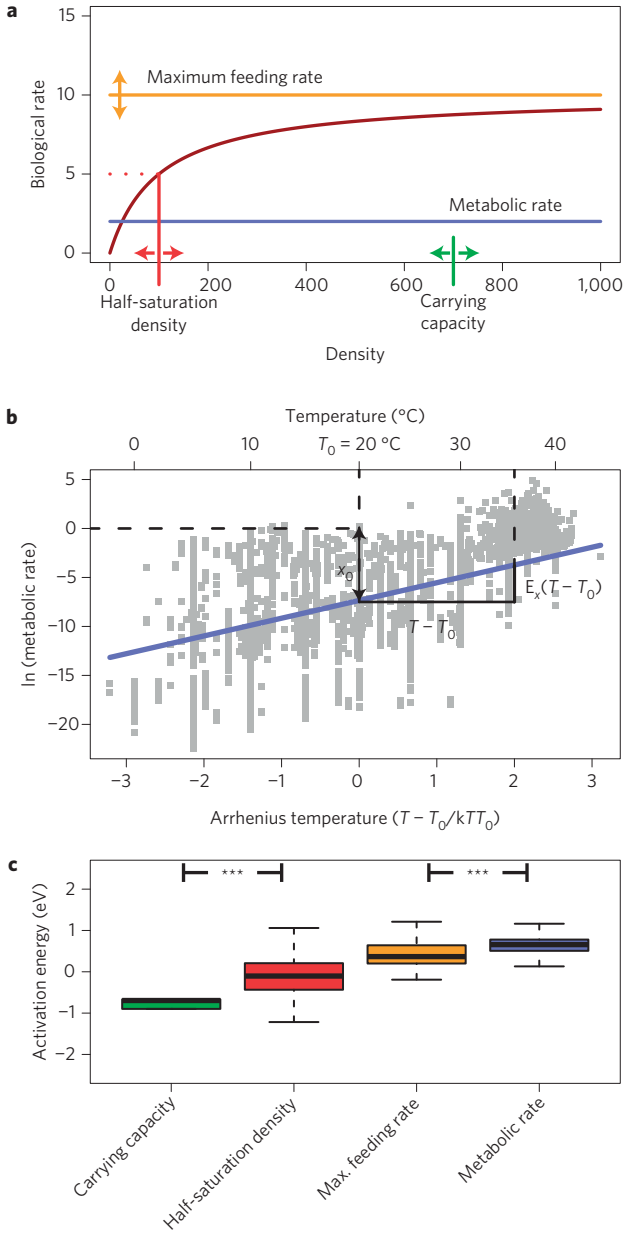

Figure 1 | Empirical warming effects on biological rates.a, Conceptual illustration of how temperature affects the parameters maximum feeding, half-saturation density (foraging inefficiency), carrying capacity (maximum prey density) and metabolic rate. The brown line shows the realized feeding rate. The vertical part of the red line shows the half-saturation density and the horizontal dashed part illustrates that at this prey density the half-maximum feeding rate is realized. **b**, Temperature scaling of metabolic rates as an illustration of activation energies (E_x) in Arrhenius equations. **c**, E_x for carrying capacity (mean = −0.77; s.d. = 0.36), half-saturation density (mean = −0.12; s.d. = 0.53), maximum feeding rate (mean = 0.47; s.d. = 0.44) and metabolic rate (mean = 0.64; s.d. = 0.29) in our empirical databases. Stars denote significant differences (***, $p < 0.001$) between pairs of rates as determined by *F*-tests (metabolic rate versus maximum feeding; carrying capacity versus half-saturation density).

the average activation energies, our analyses indicate the general pattern that within the persistence range, increasing temperatures cause decreasing amplitudes of population oscillations—thus stabilizing predator–prey systems from limit cycle (Fig. 2b) into equilibrium dynamics (Fig. 2d). Although warming increases per-unit biomass flux rates, the much stronger metabolic acceleration

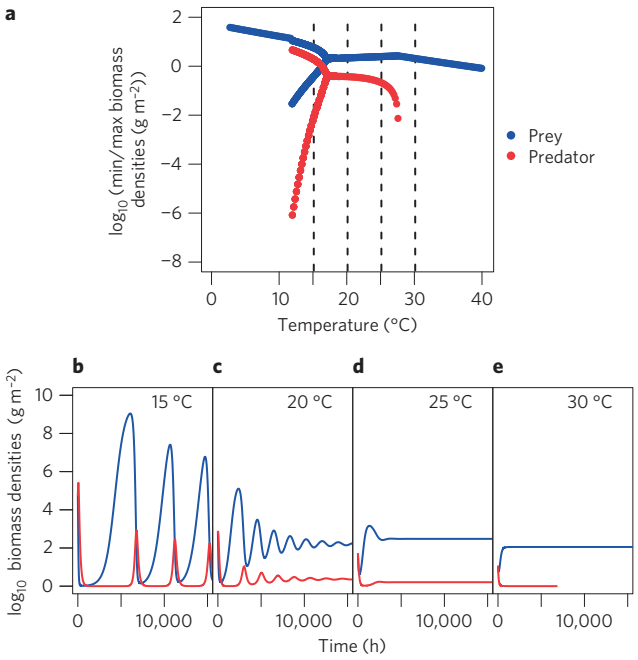

Figure 2 | Simulated predator–prey dynamics across temperature gradients.a, Bifurcation diagram showing the minimum and maximum predator and prey densities within time series across a temperature gradient. Dashed lines indicate the temperatures corresponding to the exemplary time series. **b**–**e**, Exemplary time series at 15 °C, 20 °C, 25 °C and 30 °C. To allow comparisons with empirical data **b**–**e** show the first part of the time series including transient dynamics, whereas the bifurcation diagram (**a**) shows minima and maxima within the last tenth of the simulation representing long-term dynamics. The corresponding longer time series are shown in the Supplementary Information. Blue, prey densities; red, predator densities.

(Fig. 1c) leads to lower consumer biomass densities and eventually reduces population-level fluxes. Furthermore, a decline in prey densities (carrying capacities) that is stronger than the decrease in half-saturation densities (Fig. 1c) and the associated increase in foraging efficiencies also lowers the population-level fluxes. Consequently, these two main effects cause dampened oscillations due to lower top-down pressure and higher risk of predator starvation as a consequence of lower bottom-up energy supply[20]. Thus, warming reduces population energy fluxes and leads to dynamics that are similar to an inverse paradox of enrichment[21].

To generalize our findings we replicated the simulations with one million random combinations of activation energies (normal distributions with mean values and standard deviations of our meta-analyses, see Fig. 1; resource intrinsic growth rate: 0.84 eV ±0.4; in Supplementary Table 1). *A posteriori*, we categorized the different outcomes according to the following aspects: whether predator–prey dynamics were stabilized or destabilized in terms of their coefficient of variation in biomass; and whether predators persisted or became extinct with increasing temperature (Fig. 3a). The full factorial combination of these aspects resulted in four categories that were distinguished by the distribution of the four activation energies (Fig. 3b). In contrast to previous predictions that an increase in temperature should destabilize predator–prey oscillations[3], most parameter combinations (91.1%, Fig. 3a) led to positive relationships between population stability and warming. Within this group, predators survived at high temperatures, in only 17.5% of all simulations, whereas the combination of stabilizing warming effects and predator extinction at high temperatures occurred in 73.8%—thus highlighting the broad generality of our warming predictions. Notably, only a marginal minority of all simulations

(8.9%) supported the present paradigm that warming destabilizes population dynamics (Fig. 3, see Supplementary Figs 1–4 for time series and bifurcation diagrams). The varying dynamic consequences of warming (Fig. 3a) can be explained by different combinations of activation energies (Fig. 3b). If activation energies of half-saturation densities are lower than those of carrying capacities, warming will destabilize predator–prey dynamics (Fig. 3: both left columns), as predators become more efficient and exert a stronger top-down pressure. In the opposite case, if activation energies of carrying capacities are lower than those of half-saturation densities, top-down pressure is weakened and energy fluxes are reduced and thus warming will stabilize population oscillations (Fig. 3: both right columns). In the latter case of stabilized systems, predator extinctions occur if activation energies of metabolic rates are higher than those of maximum feeding (Fig. 3, right column), thus supporting our hypothesis of predator starvation due to energetic mismatch. Despite the strong response of empirical carrying capacities to warming (Fig. 1c), our model analyses suggest that they have only marginal effects on population stability and predator persistence, because their distribution was similar across the four stability categories (Fig. 3b). Overall, our interpretation is consistent with the principle of energy flux, stating that processes (here, warming) decreasing the energy flux to consumers (here, feeding) relative to their loss rate (here, metabolic rates) will stabilize population dynamics[20]. Our results also show that continuing these processes may lead to consumer starvation. Moreover, stability implications of warming may interact with the size structure of the community[19,22] that modifies energy flux patterns[4]. In this context, our results bridge the gap between physiological warming studies and analyses of population stability to provide a mechanistic explanation for possible consequences of warming while stressing population stability and predator extinction as the most likely outcome.

Our approach is based on some limiting assumptions. First, we included only invertebrates (mainly arthropods) in our empirical databases (Fig. 1c) and model analyses (Figs 2, 3), because they represent most extant species. Although studies of vertebrate activation energies revealed similar patterns in activation energies[1,23], conclusions for endotherms may differ from our results. Second, we employed random combinations of activation energies in our model analyses (Fig. 3a), because only very few studies measured the activation energies of feeding and metabolic rate for the same species[14,24]. These studies also documented very small activation energies of half-saturation densities and that metabolic rate increases more strongly with temperature than feeding. Accordingly, they represent the fourth category with population stabilization and predator extinction (Fig. 3, right-most column), which supports the conclusions of our model analyses. However, our results also indicate the need to further study differences in temperature scaling for biological rates measured for the same species. Third, the empirical data in our databases are founded on short-term experiments excluding evolutionary responses to temperature changes that are beyond the scope here. Here we offer a framework that future studies can use for disentangling evolutionary from ecological consequences of warming. Fourth, we followed previous studies[11,23] in assuming Arrhenius scaling of the biological processes with temperature, whereas they may systematically break down at critically high temperature thresholds leading to hump-shaped temperature scalings[13,14,25]. Although these hump-shaped relationships should cause extinctions when critically high temperature thresholds are crossed[25], our results suggest that extinctions may occur even within the physiologically benign temperature range as a consequence of predator starvation despite abundant resources. Despite these limiting assumptions, our database and model analyses are offering new testable predictions for how predator–prey systems should respond to warming.

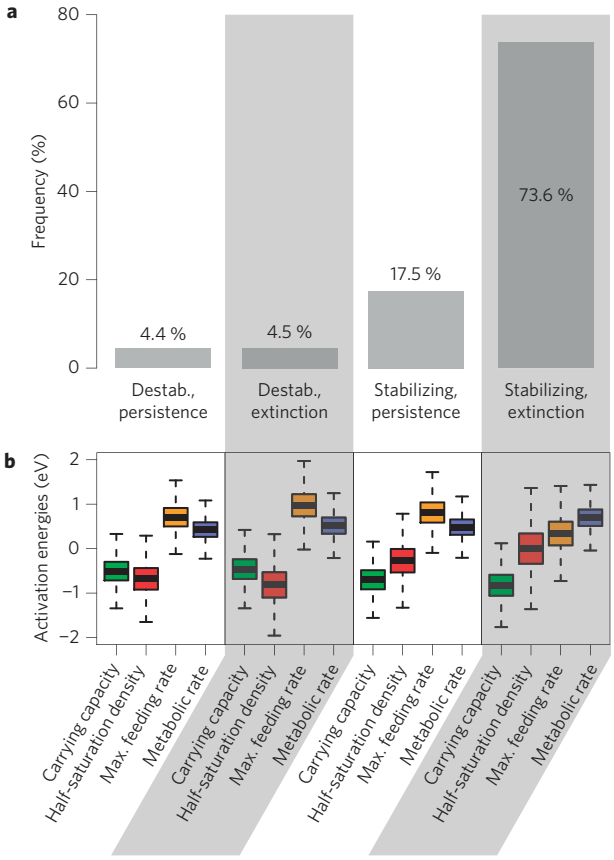

Figure 3 | Population stability and extinctions in simulated predator–prey systems.a, Percentages of possible dynamical outcomes of the simulations. Destabilizing refers to an increase of the coefficient of variation of biomass, stabilizing to a decrease. Persistence and extinction were measured at 40 °C for the predator species. **b**, Box plot of activation energies corresponding to the categories of the dynamical outcomes shown in **a**. Outliers were excluded for graphical reasons.

We tested these predictions by measuring time series along a temperature gradient from 15 °C to 30 °C in a microbial predator–prey system with *Tetrahymena pyriformis* preying on *Pseudomonas fluorescens* (see Methods for detailed laboratory and statistical methods)[26,27]. Our model analyses were based on biomass dynamics, whereas we counted abundances in the microbial experiment. As cell sizes were not affected by our temperature treatments (ANOVA, $p = 0.7198$) the data can be compared. Our results suggest a dampening of population oscillations with warming: although predator and prey populations showed strong oscillations at 15 °C (Fig. 4a), they were dampened at higher temperatures (20 °C, Fig. 4b). At 25 °C (Fig. 4c), two alternative states occurred: in two of three replicates ciliate predators persisted with both species showing lower oscillation amplitudes (Fig. 4c, Supplement Fig. 5c and g), whereas in the third replicate the predator population became extinct (Supplement Fig. 5k). At this temperature, the fragile predator–prey system was on the verge between persistence and extinction. At 30 °C (Fig. 4d), predators in all treatments became extinct. Statistically, minima and maxima of bacteria both decreased from 15 °C to 25 °C with maxima showing a steeper decrease than minima ($E_{\min,t=0} = -0.53$, $p < 0.001$; $E_{\max,t=0} = -0.64$, $p < 0.001$). Ciliate minima increased and their maxima decreased ($E_{\min,t=0} = 0.27, p < 0.001$; $E_{\max,t=0} = -0.50, p < 0.001$). These statistically significant patterns in the activation energies of minima and maxima demonstrated that the amplitudes of the predator and the prey oscillations decreased with warming (Fig. 4e).

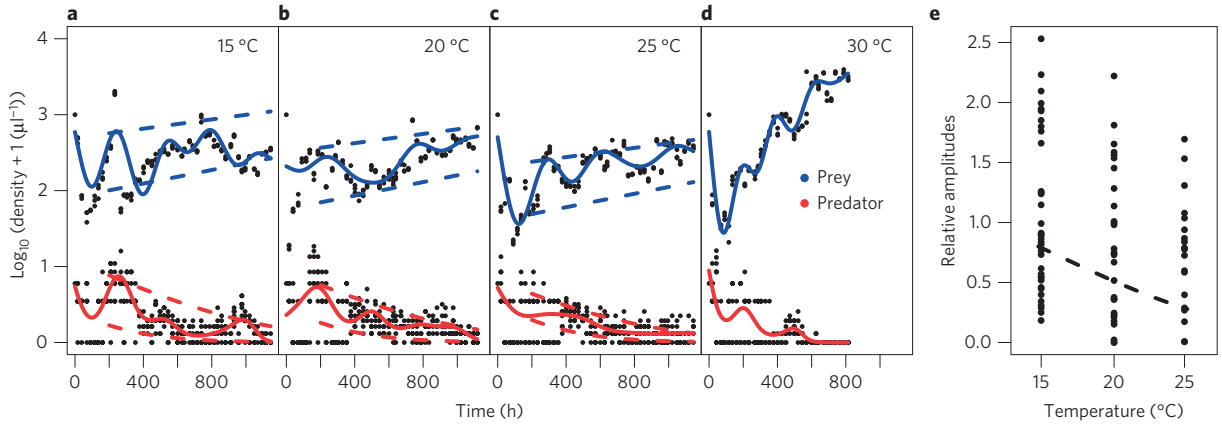

Figure 4 | Laboratory time series of the predator *T. pyriformis* (red lines) and its prey *P. fluorescens* CHA19-GFP (blue lines). a–d, Replicates of the time series at 15 °C, 20 °C, 25 °C and 30 °C were fitted with a GAM with a Poisson distribution. Dashed lines in the related colours show quantile regressions indicating the minima and maxima of abundances. **e**, Relative amplitudes of both predator and prey time series dependent on temperature. The dashed line denotes the regression line according to an average amplitude sequence number (which is 4); see Supplementary Information for details.

The experimental data thus confirmed the model predictions that warming stabilizes predator–prey dynamics by dampened oscillations, whereas predators become extinct at high temperatures.

Our analyses of global databases, model simulations and empirical microcosm experiments show that warming generally stabilizes population dynamics in predator–prey systems on ecological timescales. This is due to a mismatch between metabolic rate and realized feeding caused by: constant foraging efficiencies (that is, half-saturation densities) while prey densities (that is, carrying capacities) decrease; and increases in metabolic rate exceeding those of maximum feeding rates. Beyond a threshold temperature, the decreasing energetic efficiency with warming will cause extinction of predators owing to starvation. This contrasts with the present paradigm that warming causes extinctions by increased oscillations[3]. Our results provide evidence that populations on the verge of extinction are characterized by minimal oscillations or even equilibrium dynamics. Thus, our results increase the predictability of warming effects and illustrate the risk of predator extinction waves in a warmed world.

Methods

Database. We used published databases on metabolic rates[28,29] and functional response parameters[14] and extended them by protozoan metabolic rates and maximum population densities (Supplementary Information). Only data sets containing three or more temperature levels differing by two or more degrees Kelvin were included. To analyse data only within the biologically relevant temperature range[12] we deleted the lowest and/or highest measurements in cases where hump-shaped deviations occurred. We carried out an ordinary least-squares regression on each data set to obtain activation energies (see Supplementary Information for details).

Simulations. Consistent with previous model studies[3,4,17–19], we used a bioenergetic population model for the simulations where the biomass changes (B'_{prey} and $B'_{predator}$) follow

$$B'_{prey} = GB_{prey} - B_{predator}F \quad (2)$$

$$B'_{predator} = \varepsilon B_{predator}F - xB_{predator} \quad (3)$$

where B_{prey} and $B_{predator}$ are the biomass densities of the prey and the predator species, respectively. G is the resource's logistic growth term, F is the feeding term, ε is the assimilation efficiency and x is the predator's metabolic rate (see Supplementary Information for details). As in previous biomass models, biomass loss due to metabolic rate (biomass loss of individuals) or mortality (loss of individuals) is not differentiated.

Organisms and culture conditions. We used as bacterial prey *P. fluorescens* CHA19, a gacS-isogenic mutant of *P. fluorescens* CHA0, chromosomally tagged with green fluorescent protein[26] (GFP). This strain does not produce secondary metabolites, which allows monitoring of trophic interactions without toxin-related interferences. Bacterial stocks were kept frozen at −8 °C. Before the experiment, bacteria were grown on lysogeny broth plates supplemented with 25 µg ml^{-1} kanamycin. One single colony was picked and cultured overnight at 20 °C in liquid lysogeny broth, collected by centrifugation (13,000 r.p.m., 10,000 g for one minute) and washed three times in 1:10 modified Ornston and Stanier minimal medium supplemented with 1 mM glycerol as sole carbon source.

As predators we used the bacterivorous protozoa *T. pyriformis* CCAP 1630/1W. Protozoa were kept in axenic cultures in proteose peptone yeast extract medium containing 20 g proteose peptone and 2.5 g yeast extract per litre at 14 °C for at least five days until reaching sufficient concentrations. Before the experiments, protozoa were collected by gentle centrifugation three times (300 r.p.m., 400 g, 0 °C, for seven minutes) and resuspended in 1:10 Ornston and Stanier 1 mM glycerol medium.

Time-series experiments. Time-series experiments were conducted in 100 ml Ornston and Stanier 1:10 0.1 mM glycerol in 250 ml Erlenmeyer borosilicat glass flasks closed with aluminium caps. Flasks were incubated in thermostatic cabinets (Lovibond, Tintometer GmbH) with agitation (200 r.p.m.) at 15 °C, 20 °C, 25 °C and 30 °C. Start concentrations of *P. fluorescens* CHA19-GFP were 1,000 cells per microlitre, whereas *T. pyriformis* concentrations were 5 cells per microlitre in each treatment. Every day, 10 ml of the culture were removed for analysis and replaced with fresh medium. Bacterial counts were determined in a C6 flow cytometer (Accuri) from three 150 µl aliquots. Bacteria were gated on the basis of their SSC-A x FL1-A signal; 50,000 events per sample were recorded. If counts exceeded 5,000 events per second, samples were diluted accordingly. *T. pyriformis* were counted in an improved Neubauer (>10 cells per microlitre) or a Fuchs-Rosenthal (<10 cells per microlitre) counting chamber.

Time-series analysis. We analysed each time series through generalized additive models[30] (GAMs) and generalized linear models to analyse both the amplitude and general average trend of the times series. As populations are integers and our data showed overdispersion, we used quasipoisson models. Subsequently, we simulated 1,000 data points for each time series according to the single model results through the predict function in R. We divided the results of the GAM model by the results of the generalized linear model to calculate the normalized time-series values. We subsequently analysed at what time-step extrema of the population densities occurred[31] and calculated the resulting normalized amplitudes. We added the corresponding sequence number of the amplitude within an independent time series for further analyses (that is, amplitude 1, amplitude 2). Amplitude strength was analysed using ln-transformed normalized amplitudes as a function of sequence number, Arrhenius temperature and squared Arrhenius temperature and the interaction between both temperature terms with the amplitude sequence number. To ensure independence of data, we used linear mixed-effects models[32] with time-series identity and nested taxonomic group as random effects as well as a temporal correlation of the dependence of amplitudes to amplitude sequence number (corAR1())[33]. We selected models according to the penalized log-likelihood (Akaike's Information Criterion) using maximum likelihood (method = ML) while subsequently testing the resulting model again with the restricted estimates maximum likelihood method (method = REML)[33].

Furthermore, we analysed how minima and maxima of these predicted average time series behave with temperature and time for systems where the predator survived and systems where the predator went extinct by using the quantile regression at a level of 0.05 and 0.95 (function qr in R). To avoid transient dynamic effects, we deleted the first 200 h from the predicted values.

Received 5 March 2013; accepted 14 January 2014; published online 26 February 2014

References

1. Brown, J. H., Gillooly, J. F., Allen, A. P., Savage, V. M. & West, G. B. Toward a metabolic theory of ecology. *Ecology* **85,** 1771–1789 (2004).
2. Petchey, O. L., McPhearson, P. T., Casey, T. M. & Morin, P. J. Environmental warming alters food-web structure and ecosystem function. *Nature* **402,** 69–72 (1999).
3. Vasseur, D. A. & McCann, K. S. A mechanistic approach for modeling temperature-dependent consumer-resource dynamics. *Am. Nat.* **166,** 184–198 (2005).
4. Otto, S. B., Rall, B. C. & Brose, U. Allometric degree distributions facilitate food-web stability. *Nature* **450,** 1226–1229 (2007).
5. Parmesan, C. Ecological and evolutionary responses to recent climate change. *Annu. Rev. Ecol. Evol. Syst.* **37,** 637–669 (2006).
6. *IPCC Climate Change 2007: The Physical Science Basis* (eds Solomon, S. *et al.*) (Cambridge Univ. Press, 2007).
7. Parmesan, C. & Yohe, G. A globally coherent fingerprint of climate change impacts across natural systems. *Nature* **421,** 37–42 (2003).
8. Thomas, C. D. *et al.* Biodiversity conservation—Uncertainty in predictions of extinction risk—Effects of changes in climate and land use—Climate change and extinction risk—Reply. *Nature* **430,** http://dx.doi.org/http://dx.doi.org/10.1038/nature02719 (2004).
9. Thomas, C. D., Franco, A. M. A. & Hill, J. K. Range retractions and extinction in the face of climate warming. *Trends Ecol. Evol.* **21,** 415–416 (2006).
10. Rall, B. C., Vucic-Pestic, O., Ehnes, R. B., Emmerson, M. & Brose, U. Temperature, predator–prey interaction strength and population stability. *Glob. Change Biol.* **16,** 2145–2157 (2009).
11. Dell, A. I., Pawar, S. & Savage, V. M. Systematic variation in the temperature dependence of physiological and ecological traits. *Proc. Natl Acad. Sci. USA* **108,** 10591–10596 (2011).
12. Savage, V., Gillooly, J., Brown, J., West, G. & Charnov, E. Effects of body size and temperature on population growth. *Am. Nat.* **163,** 429–441 (2004).
13. Englund, G., Ohlund, G., Hein, C. L. & Diehl, S. Temperature dependence of the functional response. *Ecol. Lett.* **14,** 914–921 (2011).
14. Rall, B. C. *et al.* Universal temperature and body-mass scaling of feeding rates. *Phil. Trans. R. Soc. B* **367,** 2923–2934 (2012).
15. Boit, A., Martinez, N. D., Williams, R. J. & Gaedke, U. Mechanistic theory and modelling of complex food-web dynamics in Lake Constance. *Ecol. Lett.* **15,** 594–602 (2012).
16. Schneider, F. D., Scheu, S. & Brose, U. Body mass constraints on feeding rates determine the consequences of predator loss. *Ecol. Lett.* **15,** 436–443 (2012).
17. Yodzis, P. & Innes, S. Body size and consumer-resource dynamics. *Am. Nat.* **139,** 1151–1175 (1992).
18. Brose, U., Williams, R. J. & Martinez, N. D. Allometric scaling enhances stability in complex food webs. *Ecol. Lett.* **9,** 1228–1236 (2006).
19. Binzer, A., Guill, C., Brose, U. & Rall, B. C. The dynamics of food chains under climate change and nutrient enrichment. *Phil. Trans. R. Soc. B* **367,** 2935–2944 (2012).
20. Rip, J. M. K. & McCann, K. S. Cross-ecosystem differences in stability and the principle of energy flux. *Ecol. Lett.* **14,** 733–740 (2011).
21. Rosenzweig, M. L. Paradox of enrichment: destabilization of exploitation ecosystems in ecological time. *Science* **171,** 385–387 (1971).
22. Brose, U. *et al.* Climate change in size-structured ecosystems.. *Phil. Trans. R. Soc. B* **367,** 2903–2912 (2012).
23. Gillooly, J. F. B. Effects of size and temperature on metabolic rate. *Science* **293,** 2248–2251 (2001).
24. Vucic-Pestic, O., Ehnes, R. B., Rall, B. C. & Brose, U. Warming up the system: Higher predator feeding rates but lower energetic efficiencies. *Glob. Change Biol.* **17,** 1301–1310 (2011).
25. Pörtner, H. O. & Knust, R. Climate change affects marine fishes through the oxygen limitation of thermal tolerance. *Science* **315,** 95–97 (2007).
26. Jousset, A., Lara, E., Wall, L. G. & Valverde, C. Secondary metabolites help biocontrol strain *Pseudomonas fluorescens* CHA0 to escape protozoan grazing. *Appl. Environ. Microbiol.* **72,** 7083–7090 (2006).
27. Zuber, S. *et al.* GacS sensor domains pertinent to the regulation of exoproduct formation and to the biocontrol potential of *Pseudomonas fluorescens* CHAO. *Mol. Plant. Microbe Interact.* **16,** 634–644 (2003).
28. Ehnes, R. B., Rall, B. C. & Brose, U. Phylogenetic grouping, curvature and metabolic scaling in terrestrial invertebrates. *Ecol. Lett.* **14,** 993–1000 (2011).
29. White, C. R., Phillips, N. F. & Seymour, R. S. The scaling and temperature dependence of vertebrate metabolism. *Biol. Lett.* **2,** 125–127 (2006).
30. Wood, S. N. Fast stable restricted maximum likelihood and marginal likelihood estimation of semiparametric generalized linear models. *J. R. Stat. Soc. Ser. B* **73,** 3–36 (2011).
31. Kim, D. & Oh, H.-S. EMD: Empirical mode decomposition and Hilbert spectral analysis (2013); http://cran.us.r-project.org/web/packages/EMD/index.html
32. Pinheiro, J. *et al.* NLME: linear and nonlinear mixed effects models (2013); http://cran.us.r-project.org/web/packages/nlme/index.html
33. Zuur, A. F. *Mixed Effects Models and Extensions in Ecology with R.* (Springer, 2009).

Acknowledgements

The project received financial support from the Dorothea Schlözer Programme of Göttingen University. F.S. gratefully acknowledges financial support from the German Research Foundation (BR 2315/16-1). We thank C. Guill and A. Binzer for constructive ideas and suggestions during the coding process.

Author contributions

K.E.F., U.B., B.C.R. and A.J. designed the microcosm experiment. K.E.F. conducted the experiments. Statistical procedures on time series and functional responses were carried out by B.C.R. and K.E.F. B.C.R analysed the database. F.S. wrote and analysed the bioenergetic model. All authors contributed to the manuscript.

Additional information

Supplementary information is available in the online version of the paper. Reprints and permissions information is available online at www.nature.com/reprints. Correspondence and requests for materials should be addressed to U.B.